Supporting Information for

Targeting USP18 overcomes acquired resistance in hepatocellular carcinoma by regulating NCOA4 deISGylation and ferroptosis

Shengtao Ye[1], Junxin Chen[1], Ying Zheng[1], Mengmeng He[1], Yanqiu Zhang[1], Yang Cheng[1], Yingrong Leng[1], Enyi Wu[1], Lingyi Kong[1,*], Hao Zhang[1,*]

Affiliations

[1] Jiangsu Key Laboratory of Bioactive Natural Product Research and State Key Laboratory of Natural Medicines, School of Traditional Chinese Pharmacy, China Pharmaceutical University, Nanjing 210009, China

*** Corresponding authors**

Lingyi Kong, State Key Laboratory of Natural Medicines and Jiangsu Key Laboratory of Bioactive Natural Product Research, School of Traditional Chinese Pharmacy, China Pharmaceutical University, 24 Tong Jia Xiang, Nanjing 210009, China. E-mail: cpu_lykong@126.com; Tel/Fax: +86-25-8327-1405

Hao Zhang, State Key Laboratory of Natural Medicines and Jiangsu Key Laboratory of Bioactive Natural Product Research, School of Traditional Chinese Pharmacy, China Pharmaceutical University, 24 Tong Jia Xiang, Nanjing 210009, China. E-mail: hiaaron@sina.cn; Tel/Fax: +86-25-8327-1405

20 **This file includes:**

25

Supplementary methods

GSE data processing and survival prognosis analysis

GEO2R analysis was conducted on the GSE109211 dataset (http://www.ncbi.nlm.nih.gov/geo /geo2r/) to ascertain the differential expression of USP18 or ISG15 between HCC patients who responded favorably to sorafenib treatment and those who exhibited resistance. The UALCAN database (http://ualcan.path.uab.edu/) was employed to assess the correlation between USP18 and ISG15 expression levels and prognosis in HCC patients. Additionally, the Kaplan Meier plotter database (http://kmplot.com/analysis/) was utilized to investigate the prognostic significance of NCOA4 in HCC. Hazard ratio (HR) with 95% confidence intervals was estimated along with log-rank p-value. Statistical significance was defined as $p < 0.05$ by established criteria.

Histological analyses and immunohistochemical (IHC) staining

Xenografts or liver specimens were fixed in 10% neutral buffered formalin, followed by paraffin embedding and sectioning into 4 μm slices. Subsequently, the sections underwent deparaffinization, hydration, and staining using established protocols. Histological sections were stained with hematoxylin-eosin (H&E) to evaluate the inhibitory impact of the drug on tumors. Tissue sections were subjected to Ki67 staining to evaluate the suppressive impact of drugs on tumor proliferation. IHC was performed using paraffin sections, which were incubated with the indicated primary antibodies. The sections were scanned using a NanoZoomer 2.0 RS Pathological slide scanner (C10730-13, Hamamatsu), and the images were then digitalized.

49 **Cell lines**

50 HepG2 cells and HCCLM3 cells were purchased from the Cell Bank of the Type
51 Culture Collection of the Chinese Academy of Sciences, Shanghai, China. All of
52 the cell lines were authenticated in-house by short tandem repeat (STR) DNA
53 profiling. To establish HepG2-SR and HCCLM3-SR cells, parental HepG2 or
54 HCCLM3 cells were subjected to incremental concentrations of sorafenib,
55 starting at 6 μM, until they acquired the ability to proliferate unhindered in the
56 presence of 12 μM sorafenib. This adaptation was achieved after 24 weeks
57 under continuous drug exposure. The HepG2-USP18-OE and HCCLM3-USP18-
58 OE cell lines, stably over-expressing USP18, were generated by transfecting the
59 pCMV-N-Myc-USP18 plasmid followed by G418 selection. Control cells
60 corresponding to each line were also established. Mycoplasma contamination
61 was assessed at least once per month, and the test results were negative.

62 **RNA extraction, reverse transcription PCR, and quantitative real-time PCR**

63 Total RNA was extracted from HepG2 cells, HepG2-SR cells, and HepG2-
64 USP18-OE cells using the RNA Quick Purification Kit (ES Science, Shanghai,
65 RN001) following the manufacturer's instructions. The quality and concentration
66 of the RNA were assessed by measuring absorbance at 260 and 280 nm using a
67 Thermo Scientific NanoDrop spectrophotometer. Reverse transcription of 1μg of
68 total RNA was performed using the HiScript® II Q Select RT SuperMix for qPCR
69 Kit (Vazyme, R232-01). Quantitative real-time PCR (qRT-PCR) was conducted
70 on a LightCycler480 Instrument II (Roche Diagnostics Inc., Basel, BS,
71 Switzerland) using SYBR Green qPCR Master Mix (Vazyme, Q321-02) and

72 corresponding primers listed in Table S2. The mRNA expression levels of target
73 genes were normalized to GAPDH expression. The specificity of each amplicon
74 was confirmed by analyzing its melting curve.

75 **Protein extraction, western blot analysis and co-immunoprecipitation (Co-**
76 **IP)**

77 The total protein was isolated from liver tissues and cells were harvested and
78 lysed on ice for 30 min using lysis buffer (Yeasen, 20118ES60) with protease
79 inhibitor cocktail (Beyotime, P1005) and phosphatase inhibitor cocktail (Beyotime,
80 P1045). The supernatants of lysates were collected by centrifugation at 12, 000
81 rpm for 10 min at 4 ℃, and the protein concentration was determined with a BCA
82 protein assay kit (Beyotime, catalog # P0012). Supernatants were analyzed for
83 western blot analysis or immunoprecipitation.

84 For western blot analysis, equal amounts of total protein were separated on
85 10% or 12% SDS-PAGE gels and subsequently transferred to PVDF membranes
86 (Bio-Rad). Following a blocking step with 5% skim milk for 2 h, the membranes
87 were incubated overnight at 4 ℃ with primary antibodies. Subsequently, the
88 membranes were incubated with HRP-conjugated secondary antibodies for an
89 additional 2 h. The specific antibodies used in this study are listed in the
90 materials. Immunoreactive signals were detected using an ECL kit (170-5061;
91 Bio-Rad; Hercules, CA) and visualized by chemiluminescence employing a
92 ChemiDOC XRS^{+} Molecular Imaging System (Bio-Rad). The band intensities

93 were quantified using Image J software and calculated based on reference bands
94 obtained from anti-β-actin immunoblotting.
95 For Co-IP, the prepared cell lysates containing 1 mg total protein were
96 precleared using 10 μL Protein A+G Agarose beads by rotating at 4 ℃ for 2-4 h.
97 Subsequently, the indicated antibody was added to the precleared lysates,
98 followed by the addition of 25 μL Protein A+G Agarose beads to the mixture. The
99 tubes were then rotated at 4 ℃ for a duration of 4-6 h for each process. As a
100 negative control, normal mouse or rabbit IgG was utilized. Following this step, the
101 beads underwent washing with cold PBS buffer (3-5 times) and subsequently
102 boiled with SDS loading buffer for 10 min. The immune complexes obtained were
103 collected and subjected to western blot analysis utilizing both primary antibodies
104 as indicated and corresponding secondary antibodies by established protocols.
105 **Plasmid constructs**
106 The full-length coding region of the USP18 gene was cloned into the multiple
107 cloning site (MCS) region of the pCMV-N-Myc vector to screen for HCC cell lines
108 that stably overexpress USP18. The full-length coding region of the ISG15 gene
109 was inserted into the MCS region of the pCMV-C-HA vector to investigate and
110 validate the impact of ISG15 overexpression on USP18 protein stability in HCC
111 cells. The complete coding sequence of the USP18 gene was integrated into the
112 MCS region of the pET28a(+) vector, and subsequently, USP18 IBB1 MUT
113 plasmids were generated using a mutation kit to facilitate the purification of both
114 wild-type USP18 protein and its mutant variant, USP18 IBB1 MUT protein. To

115 synthesize ISG15-AMC, the complete coding sequence of the ISG15 gene was
116 inserted into the MCS region of the pTYB21 vector. The primers used for plasmid
117 construction are listed in Table S3.

118 **Plasmid and small-interfering RNA (siRNA) transfection**

119 For plasmid or siRNA transfection, LipofectAMINE 2000 (Invitrogen) was
120 employed following the manufacturer's instructions. To achieve successful
121 overexpression or knockdown of the target gene, a mixture of 4 μg plasmid or
122 100 nM specific siRNA and 4 or 7.5 μL LipofectAMINE 2000 should be
123 thoroughly combined in Opti-MEM. Following an incubation period of 8 h post-
124 transfection, it is recommended to replace the culture medium. The assessment
125 of overexpression or knockdown efficiency can be conducted after 48 h. The
126 sequence of the antisense siRNA is listed in Table S4.

127 **Cell counting kit-8 (CCK-8), 5-ethynyl-2'-deoxyuridine (EDU), and colony**
128 **formation assay**

129 For CCK-8 assay, transfected cells were cultured in a 96-well plate at a density
130 of 8000 cells per well. Plasmid and siRNA transfection, as well as drug treatment,
131 followed established protocols. Subsequently, each well was supplemented with
132 10 μL CCK-8 solution and incubated at 37 ℃ for 2-4 h. The absorbance at 450
133 nm was measured using Spectra-Max Plus 384 (Molecular Devices) to quantify
134 cell viability.

135 For EDU assay, cells were transfected in a 96-well plate at a density of 12, 000
136 cells per well. Plasmid and siRNA transfection, as well as drug treatment, were
137 performed following established protocols. Subsequently, each well was

138 supplemented with 20 μM EDU (Beyotime, C0071S) and incubated at 37 ℃ for 4
139 h. The cells were then fixed, permeabilized, and subjected to staining with
140 Hoechst 33342 to visualize the nuclei. To determine the proportion of EDU-
141 positive cells, cell counts were conducted in three randomly selected areas within
142 each well.

143 For the colony formation assay, the transfected cells were seeded at a density
144 of 1, 000 cells per well in a 6-well plate and treated with sorafenib and/or HYP for
145 24 h in complete media (2 mL). After washing with PBS, the cells were cultured
146 in complete media for an additional 14 days. The proliferating colonies were fixed
147 using 4% paraformaldehyde and stained with crystal violet.

148 **Transmission electron microscope assay**

149 Cells were collected and fixed with 2.5% glutaraldehyde, followed by post-fixation
150 in 2% tetroxide and dehydration through a series of ethanol gradients.
151 Subsequently, the samples were embedded in epoxy resin, sectioned into thin
152 slices, and placed onto nickel grids. High-resolution images were acquired using
153 a Hitachi-7500 transmission electron microscope (Hitachi, Tokyo, Japan).

154 **Determination of lipid peroxidation**

155 BODIPY 581/591 C11 (Thermo Fisher) was employed for the detection of lipid
156 peroxidation by the manufacturer's instructions. The quantification of
157 malondialdehyde (MDA) content was performed using respective biochemical
158 assay kits (Beyotime, S0131S).

159 **Measurement of total Fe^{2+} levels in HCC cells**

160 The level of Fe^{2+} was determined using FerroOrange (1 μM, MKBio, MX4559) by
161 the manufacturer's instructions. Briefly, cells were transfected in a 96-well plate
162 at a density of 12, 000 cells per well following established protocols for plasmid
163 and siRNA transfection as well as drug treatment. Subsequently, each well was
164 incubated with 1 μM FerroOrange at 37 ℃ for 30 min and then stained with
165 Hoechst 33342 to visualize the nuclei. Fluorescence intensity was analyzed
166 under an ImageXpress Micro Confocal Platform (Molecular Devices) equipped
167 with a 60x objective lens. (Abs_{max}=542 nm, FL_{max}=572 nm).

168 **Measurement of intracellular reactive oxygen species (ROS) generation**

169 Intracellular levels of ROS were quantified using the ROS assay kit (Beyotime,
170 China) through the conversion of a DCFH-DA fluorescence probe. Briefly, HCC
171 cells were transfected with plasmid or siRNA for 36 h and subsequently treated
172 with DMSO or sorafenib for 24 h. Following this, cells were incubated at a final
173 concentration of 10 μM DCFH-DA fluorescence probe for 20 min at 37 ℃ and
174 stained with Hoechst 33342 to visualize the nuclei. Finally, fluorescence intensity
175 was analyzed under an ImageXpress Micro Confocal Platform (Molecular
176 Devices) equipped with a 60x objective lens.

177 **Cellular thermal shift assay (CETSA)**

178 Briefly, HepG2-USP18-OE cells were seeded in 10 cm culture dishes and
179 cultured until reaching a confluence of 70-80%. Subsequently, the cells were
180 treated with 40 μM HYP or DMSO for 4 h. The cells were then collected, pelleted,
181 and washed with PBS before being resuspended to a density of 5×10^6 cells/mL

182 in PBS supplemented with protease inhibitor. Following this, 100 μL of each cell
183 suspension was dispensed into PCR tubes and subjected to thermal cycling at
184 temperatures ranging from 42-56 ℃ for 3 min. The cells were immediately lysed
185 by freeze-thawing in liquid nitrogen after heating. To clarify the cell lysates,
186 centrifugation was performed at a speed of 20, 000 g for 20 min at a temperature
187 of 4 ℃. Finally, the supernatants obtained were analyzed through Western blot.

188 **ISG15-AMC hydrolysis assay**

189 ISG15-AMC hydrolysis assay was performed to determine the inhibitory effect of
190 compounds on USP18 enzyme activity. Excess-free AMC in the samples was
191 removed by dialyzing in ISG15-AMC reaction buffer (50 mM Tris, 250 mM NaCl,
192 pH 7.5). Candidate compounds were accurately weighed and dissolved in DMSO
193 to prepare a 1 mM solution for subsequent use. Each reaction consisted of 0.5
194 μL compound sample, 2.5 μL prepared USP18 enzyme solution, and 19.5 μL
195 reaction buffer (50 mM Tris-HCl, 1 mM EDTA, 1 mM ATP, 5 mM $MgCl_2$, 1 mM
196 DTT, 1 mg/mL Ovalbumin, pH 7.5), which was incubated at a temperature of
197 37 ℃ for 5 min before adding 2.5 μL ISG15-AMC. A positive control well
198 (replacing the compound sample with 0.5 μL DMSO) and a blank substrate well
199 (replacing the USP18 with an equal volume of 2% DMSO) were set up
200 simultaneously. The reaction progress was monitored using SpectraMax
201 Paradigm Multi-Mode Detection Platform (Molecular Devices) equipped with an
202 optical module operating at an excitation wavelength of 380 nm and emission
203 wavelength of 460 nm. Measurements were taken every 20 s for a total duration

204 of 10 min. The inhibition rate of USP18 enzyme activity was calculated based on

205 the derived reaction rate obtained from enzymatic activity measurements.

206

207 **Supplementary materials**

Reagent or Resource	Source	Identifier
Antibodies		
anti-USP18, WB, dil:1/1000; IP, dil: 1/50	Cell Signaling Technology	Cat# 4813; RRID: AB_10614342
anti-ubiquitin, WB, dil: 1/1000	Cell Signaling Technology	Cat# 20326; RRID: AB_3064918
anti-Myc tag, WB, dil: 1/1000	Cell Signaling Technology	Cat# 2276; RRID: AB_331783
anti-TBK1, WB, dil: 1/1000	Cell Signaling Technology	Cat# 3504; RRID: AB_2255663
anti-pTBK1, WB, dil: 1/1000	Cell Signaling Technology	Cat# 5483; RRID: AB_10693472
anti-IRF3, WB, dil: 1/1000	Cell Signaling Technology	Cat# 4302; RRID: AB_1904036
anti-pIRF3, WB, dil: 1/1000	Cell Signaling Technology	Cat# 4947; RRID: AB_823547
anti-NCOA4, WB, dil:1/1000; IP, dil: 1/100	Abcam	Cat# ab86707; RRID: AB_1925236
anti-USP18, IHC, dil:1/100	Abclonal	Cat# A16739; RRID: AB_2772822
anti-NCOA4, IHC, dil: 1/100	Aifang Biological	Cat# AF04009;
anti-ISG15, WB, dil:1/1000	Proteintech	Cat# 15981-1-AP; RRID: AB_2126302
anti-β-Actin, WB, dil: 1/1000	Proteintech	Cat# 20536-1-AP; RRID: AB_10700003
anti-HA tag, WB, dil: 1/1000	YEASEN	Cat# 30702ES60; RRID: AB_2920545
anti-normal rabbit IgG, IP, 2μg	Cell Signaling Technology	Cat# 2729; RRID: AB_1031062
anti-mouse IgG control, IP, 2μg	Cell Signaling Technology	Cat# 5415; RRID: AB_10829607
Peroxidase AffiniPure Goat Anti-Mouse IgG(H+L), WB, dil: 1/10000	YEASEN	Cat# 33201ES60; RRID: AB_10015289

Continued		
Reagent or Resource	**Source**	**Identifier**
Peroxidase AffiniPure Goat Anti-Rabbit IgG(H+L), WB, dil: 1/10000	YEASEN	Cat# 34201ES60; RRID: AB_10015282
Experimental models: Cell lines		
HepG2	Cell bank of CAS	N/A
HCCLM3	Cell bank of CAS	N/A
HepG2-SR	This paper	N/A
HCCLM3-SR	This paper	N/A
HepG2-USP18-OE	This paper	N/A
HCCLM3-USP18-OE	This paper	N/A
Competent cells: DH5α	GENERAL BIOL	N/A
Competent cells: BL21	GENERAL BIOL	N/A
Experimental models: Organisms/strains		
BALB/c Nude mice	Vital River Laboratory	N/A
C57BL/6J mouse	Vital River Laboratory	N/A
Biological samples		
HCC tissues microarray	LD BIO	Cat# LVC1609
Plasmid		
N-Ras	Addgene	Cat# 14723
C-myc	Addgene	Cat# 102625
Sleeping Beauty transposase	Addgene	Cat# 34879
pET-28a(+)	Addgene	Cat# 69864
pCMV-C-HA	Beyotime	Cat# D2639
pCMV-N-Myc	Beyotime	Cat# D2756
pCMV-N-mCherry	Beyotime	Cat# D2711
pTYB21	NEB	Cat# N6709
pTYB21-ISG15	This paper	N/A
pCMV-C-HA-ISG15	This paper	N/A
pET-28a(+)-USP18	This paper	N/A
pCMV-N-Myc-USP18	This paper	N/A
pCMV-N-mCherry-FTH1	This paper	N/A
pET-28a(+)-USP18 IBB1 Mut	This paper	N/A

Continued		
REAGENT or RESOURCE	**SOURCE**	**IDENTIFIER**
Oligonucleotides		
Primer for qPCR, see Table S2	This paper	N/A
Primer for PCR, see Table S3	This paper	N/A
Primer for siRNA, see Table S4	This paper	N/A
Chemicals, peptides, recombinant proteins, and critical commercial assays		
DAPI Staining Solution	Beyotime	Cat# C1006
PMSF	Beyotime	Cat# ST506
Penicillin-Streptomycin	Beyotime	Cat# C0222
PBS	Beyotime	Cat# C0221
Crystal Violet	Beyotime	Cat#C0121
Protease inhibitor cocktail	Beyotime	Cat# P1005
Phosphatase inhibitor	Beyotime	Cat# P1081
MG-132	Beyotime	Cat# S1748
BCA protein assay kit	Beyotime	Cat# P0010
His-tag purification resin kit	Beyotime	Cat# P2226
1M Tris-HCl, pH6.8	Beyotime	Cat# ST768
1M Tris-HCl, Ph8.8	Beyotime	Cat# ST788
TEMED	Beyotime	Cat# ST728
30% ACR-Bis	Beyotime	Cat# ST003
10% APS	Beyotime	Cat# ST005
EdU Cell Proliferation Kit with Alexa Fluor 488	Beyotime	Cat# C0071
Coomassie Blue Fast Staining Solution	Beyotime	Cat# P0017
Reactive Oxygen Species Assay Kit	Beyotime	Cat# S0033
Hochest 33342	Beyotime	Cat# C1029
DAPI Staining Solution	Beyotime	Cat# C1006
DTT	Beyotime	Cat# ST043
MDA assay kit	Beyotime	Cat# S0131S
RNA Quick Purification Kit	ES Science	Cat# RN001

Continued		
REAGENT or RESOURCE	**SOURCE**	**IDENTIFIER**
Trypsin	Gibco	Cat# 27250-018
Fetal Bovine Serum (FBS)	Gibco	Cat# 16140071
DMEM	Gibco	Cat# 11885084
RPMI 1640	Gibco	Cat# 11875101
Lipofectamine 2000 Transfection Reagent	Invitrogen	Cat# 11668019
BODIPY™ 581/591 C11	Invitrogen	Cat# D3861
Protein A/G Magnetic Beads	MedChemExpress	Cat# HY-K0202
PEG300	MedChemExpress	Cat# HY-Y0873
Cell counting kit-8 (CCK-8)	MedChemExpress	Cat# HY-K0301
sorafenib	MedChemExpress	Cat# HY-10201
hyperoside	MedChemExpress	Cat# HY-N0452
Ferrostatin-1	MedChemExpress	Cat# HY-100579
ZVAD-FMK	MedChemExpress	Cat# HY-16658B
Necrostatin-1	MedChemExpress	Cat# HY-15760
H151	MedChemExpress	Cat# HY-112693
Ferrous bis-glycinate	MedChemExpress	Cat# HY-130078
EcoR Ⅰ	NEB	Cat# R0101
BamH Ⅰ	NEB	Cat# R0136
Hind Ⅲ	NEB	Cat# R0104
IPTG	Beyotime	Cat# ST098
Chitin Resin	Sangon Biotech	Cat# C500097-0005
Agarose	Sangon Biotech	Cat# A620014
Octet® Ni-NTA Biosensors	SARTORIUS	Cat# 18-5101
Glutaraldehyde Fixed Solution	Servicebio	Cat# G1102
FerroOrange (Fe^{2+} indicator)	Shanghai Maokang	Cat# MX4559
MesNa	Shanghai yuanye	Cat# S16035
Gly-AMC	Shanghai yuanye	Cat# Y70814
NHS	Shanghai yuanye	Cat# S30615
Triton X-100	Sigma-Aldrich	Cat# T8787
ECL kit	UU Bio	Cat# U10012

Continued		
REAGENT or RESOURCE	**SOURCE**	**IDENTIFIER**
FDA-Approved & Pharmacopeia Drug Library	TargetMol	Cat# L1010
HiScript III RT SuperMix for qPCR	Vazyme	Cat#R323-01
ChamQ SYBR qPCR Master Mix	Vazyme	Cat#Q341-02
HiScript II Q RT SuperMix for qPCR	Vazyme	Cat# R222
ChamQ SYBR qPCR Master Mix(Without ROX)	Vazyme	Cat# Q321
ClonExpress II One-Step Cloning Kit	Vazyme	Cat# C112
Mut Express MultiS Fast Mutagenesis Kit V2	Vazyme	Cat# 215
2 × Phanta Max Master Mix (Dye Plus)	Vazyme	Cat# P525
DNA Marker DL2000	Vazyme	Cat# MD101-01
WB/IP lysis buffer	YEASEN	Cat# 20118ES60
LysoSensor™ Green DND-189	YEASEN	Cat# 40767ES50
Software and algorithms		
Prism 8.0	GraphPad	N/A
ImageJ	Open source	N/A
Image Lab software	BIO-RAD	N/A
NDP. VIEW 2.3.1	Hamamatsu Photonic K.K.	N/A

208

209 **Supplementary Tables**

210 **Table S1. The information on the top five potential transcription factors of**

211 **ISG15, Related to Fig. 5l.**

Matrix ID	Name	Score	Relative score	Sequence ID	Start
MA1418.1	**IRF3**	**30.260056**	**0.988759**	**Hg38_knownGene_ENST00000649529.1**	**1886**
MA1596.1	ZNF460	25.988571	0.990282	Hg38_knownGene_ENST00000649529.1	1893
MA0517.1	STAT1::STAT2	21.051506	0.986147	Hg38_knownGene_ENST00000649529.1	827
MA0671.1	NFIX	9.016852	0.957786	Hg38_knownGene_ENST00000649529.1	641
MA0161.1	NFIC	8.52041	0.960578	Hg38_knownGene_ENST00000649529.1	642

212
213

214 **Table S2. Primers for qPCR, Related to Fig. 5, Fig. S5**

Genes	Forward primer (5'-3')	Reverse primer (5'-3')
human		
IFNB1	CAGCATCTGCTGGTTGAAGA	CATTACCTGAAGGCCAAGGA
IFI44	GGTGGGCACTAATACAACTGG	CACACAGAATAAACGGCAGGTA
USP18	CCTGAGGCAAATCTGTCAGTC	CGAACACCTGAATCAAGGAGTTA
ISG15	CGCAGATCACCCAGAAGATCG	TTCGTCGCATTTGTCCACCA
GAPDH	CTGGGCTACACTGAGCACC	AAGTGGTCGTTGAGGGCAATG

215
216

217 **Table S3. Primers for PCR, Related to construction of plasmid**

Genes	Forward primer (5'-3')	Reverse primer (5'-3')
human		
pTYB21-ISG15	CGCGATATCGTCGACGGATCCATGGGCTGGGACCTGACGGT	TTAATTACCTGCAGGGAATTCGCTCCGCCCGCCAGGCTCTG
pCMV-C-HA-ISG15	CGCTCTAGCCCGGGCGGATCCATGGGCTGGGACCTGACGGT	ATCGAATTCCTGCAGAAGCTTGCTCCGCCCGCCAGGCTCTG
pET-28a(+)-USP18	CAGCAAATGGGTCGCGGATCCATGAGCAAGGCGTTTGGGCT	TTGTCGACGGAGCTCGAATTCGCACTCCATCTTCATGTAAA
pET-28a(+)-USP5	CAGCAAATGGGTCGCGGATCCATGGCGGAGCTGAGTGAGGA	TTGTCGACGGAGCTCGAATTCGCTGGCCACTCTCTGGTAGA
pET-28a(+)-USP14	CAGCAAATGGGTCGCGGATCCATGCCGCTCTACTCCGTTAC	TTGTCGACGGAGCTCGAATTCCTGTTCACTTTCCTCTTCCA
pET-28a(+)-USP16	CAGCAAATGGGTCGCGGATCCATGGGAAAGAAACGGACAAA	TTGTCGACGGAGCTCGAATTCCAGTATTCTCTCATAAAATA
pCMV-N-Myc-USP18	GATCTGAGCCCGGGCGGATCCATGAGCAAGGCGTTTGGGCT	TCTGTCGACGATATCGAATTCGCACTCCATCTTCATGTAAA
pET-28a(+)-USP18 ALA141 A/Q	TCAACAACTGTACCGCAAACTCTGGAACCTGATTAAGGACCA	TGCGGTACAGTTGTTGAGCATCATGTTGGACAAACAAGGGC
pET-28a(+)-USP18 SER197 S/Q	CCCACTTCAACTTTTTGATGTGGACTCAAAGCCCCTGAAG	CAAAAAGTTGAAGTGGGAGGGTGAGCATGCTGCTGTTTCT
pET-28a(+)-USP18 HIS255 H/Q	GACAATCCAACTCATGCGATTCTCCATCAGGAATTCACAGACG	GCATGAGTTGGATTGTCAGGGTCTGGGGCAAATGGGTC

pCMV-N-mCherry-FTH1	GACGAGCTGTACAAGGG ATCCATGACGACCGCGT CCACCTC	TCTGTCGACGATATCGAA TTCGCTTTCATTATCACT GTCTC

218
219

220 **Table S4. sequence of siRNA**

	Sequence for siRNA(5'-3')
USP18 siRNA-1	CCAGGGAGTTATCAAGCAA
USP18 siRNA-2	CATCCGGAATGCTGTGGAT
ISG15 siRNA-1	GCACCGUGUUCAUGAAUCUUU
ISG15 siRNA-2	GCAACGAAUUCCAGGUGUC
NCOA4 siRNA-1	CCCAGGAAGTATTACTTAATT
NCOA4 siRNA-2	GCTGGCAAACAGAAGTTTAAA

221

Supplementary Figure Legends

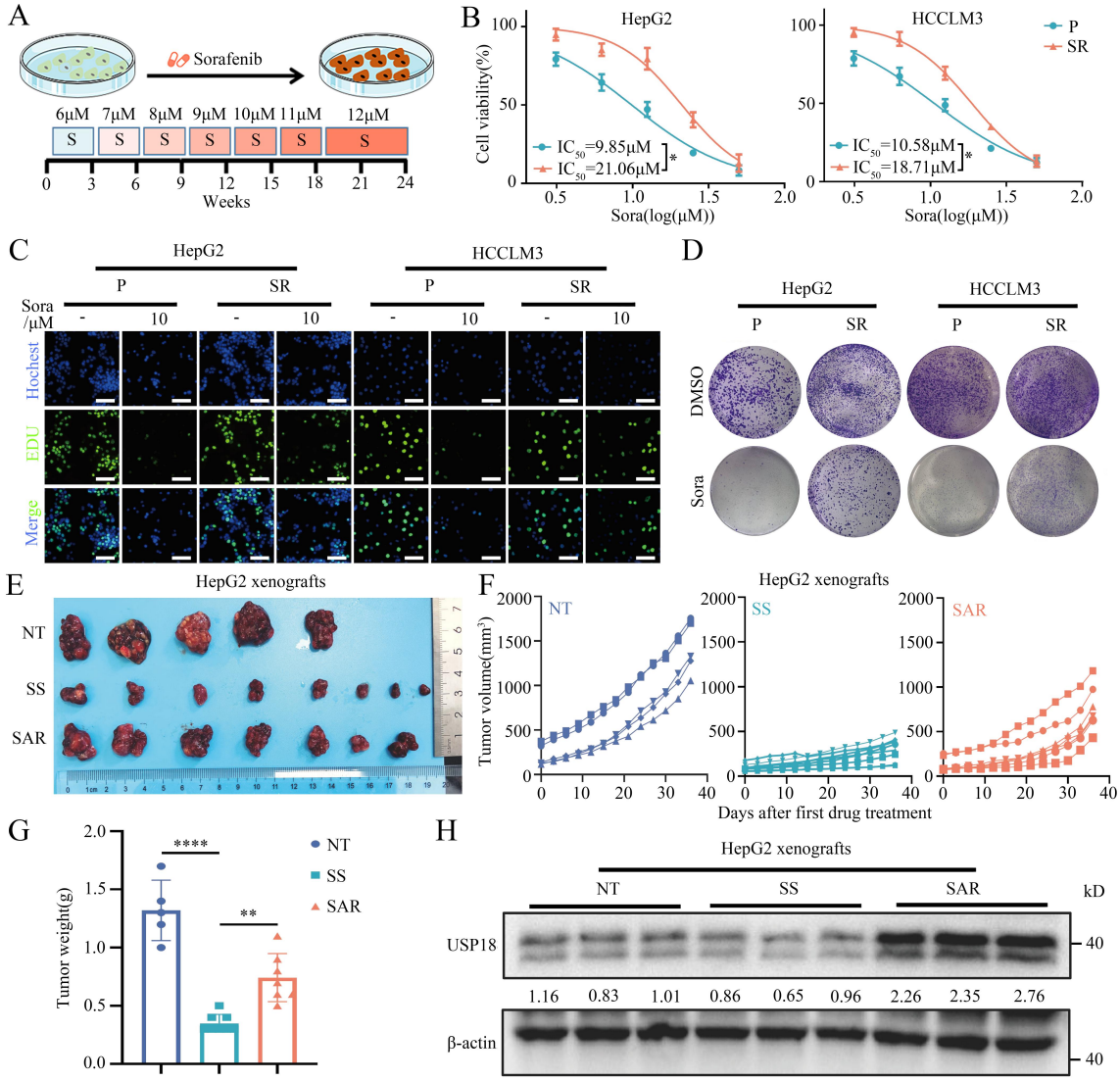

Figure S1. Construction of HCC-SR model in both *in vivo* and *in vitro* settings. (A) Schematic diagram of the establishment of HCC-SR model *in vitro*. **(B-D)** CCK-8 (B), EDU (C), and colony formation assay (D). The successful establishment of two HCC-SR cell lines (means ± SEM, *p < 0.05, paired student's t-test). **(E)** Representative pictures of subcutaneous HepG2 xenografts from the indicated groups (n ≥ 5 mice per group). **(F)** The tumor growth curve of

230 HepG2 cells in nude mice from different groups. Tumor volume was measured
231 every 3 days beginning from the first treatment. **(G)** The tumor weights from the
232 indicated groups (means ± SEM, **$p < 0.01$, ****$p < 0.0001$, one-way ANOVA
233 test). $n \geq 5$ mice per group. **(H)** Protein expression of USP18 in the HepG2
234 xenografts from the indicated groups. The intensities of bands were analyzed by
235 Image J and normalized to the mean of the corresponding NT group.
236

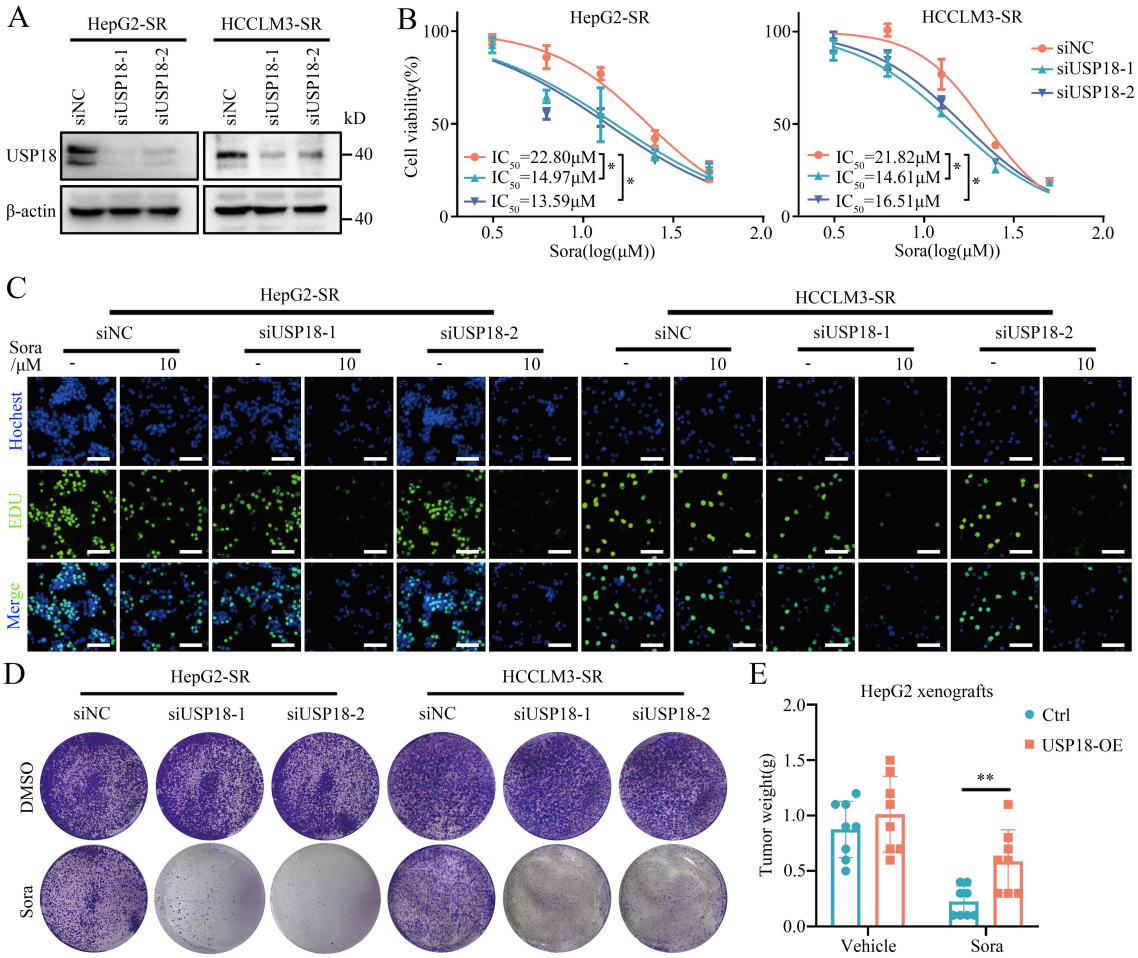

Figure S2. USP18 knockdown sensitizes HCC-SR cells to sorafenib treatment. (A) Protein expression of USP18 in HCC-SR cell lines after transfection of USP18 siRNAs for 48 h. **(B-D)** CCK-8 (B), EDU (C), and clone formation assay (D). The impact of USP18 knockdown on the susceptibility of HCC-SR cells toward sorafenib treatment (means ± SEM, *p < 0.05, one-way ANOVA test). Scale bars, 5 μm (D). **(E)** The tumor weights from the indicated groups (means ± SEM, **p < 0.01, unpaired student's t-test). n = 8 mice per group.

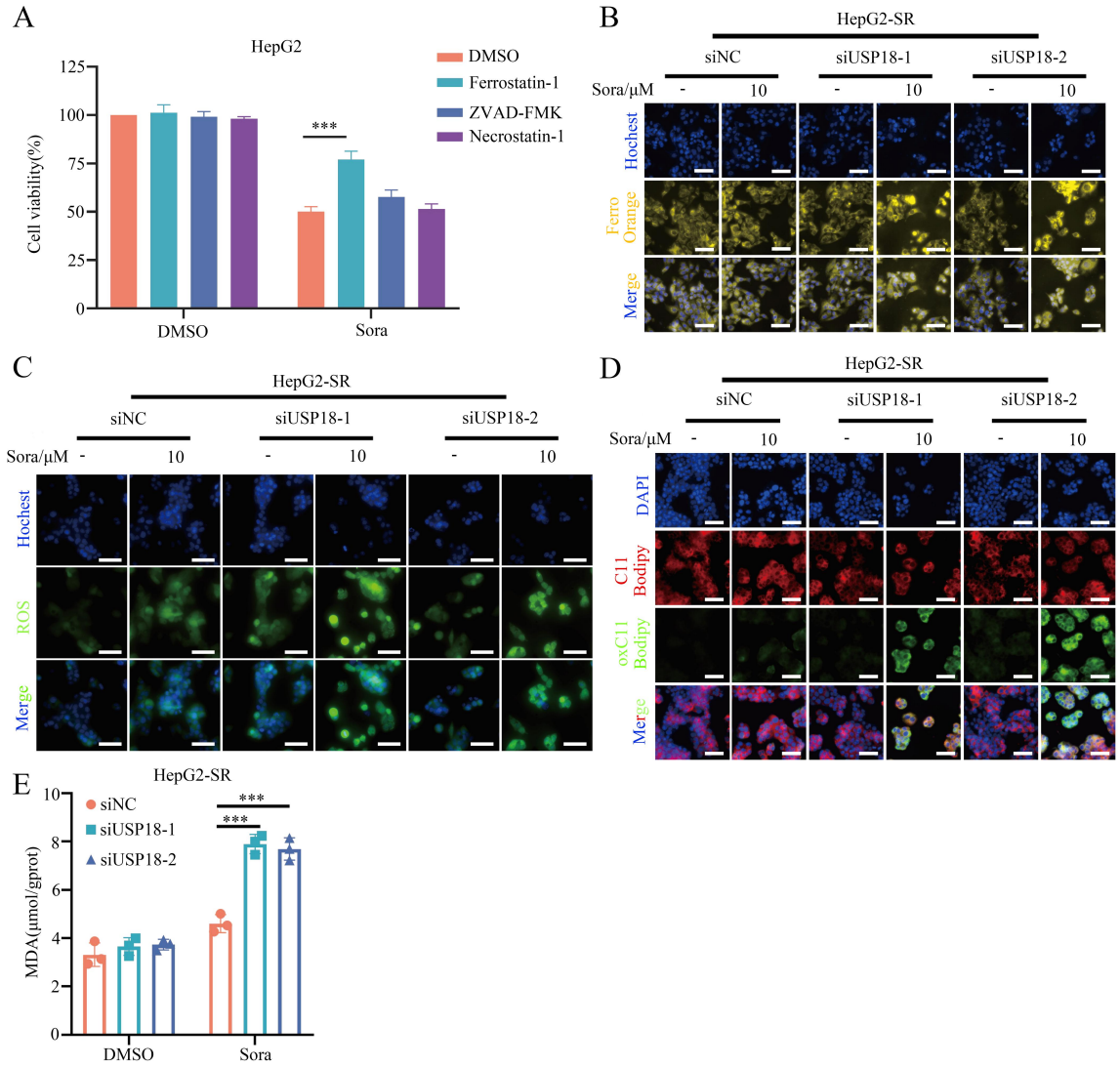

Figure S3. USP18 knockdown enhances the efficacy of sorafenib-induced ferroptosis in HCC-SR cells. (A) CCK-8 assay. HepG2 cells were treated with DMSO or 10 μM sorafenib in the absence or presence of ferrostatin-1(2 μM), Necrosulfonamide (0.5 μM), and ZVAD-FMK (10 μM) for 24 h (means ± SEM, ***$p < 0.001$, one-way ANOVA test). **(B)** FerroOrange staining. The impact of USP18 knockdown on the sorafenib-induced elevation of Fe^{2+} levels in HepG2-SR cells. Scale bars, 5 μm. **(C)** ROS staining. The effect of USP18 knockdown

254 on the generation of ROS induced by sorafenib in HepG2-SR cells. Scale bars, 5
255 μm. **(D, E)** BODIPY 581/591 C11 staining (D) and MDA assay (E). The impact of
256 USP18 knockdown on sorafenib-induced lipid peroxidation (mean ± SEM, ***$p < 0.001$, one-way ANOVA test). Scale bars, 5 μm.

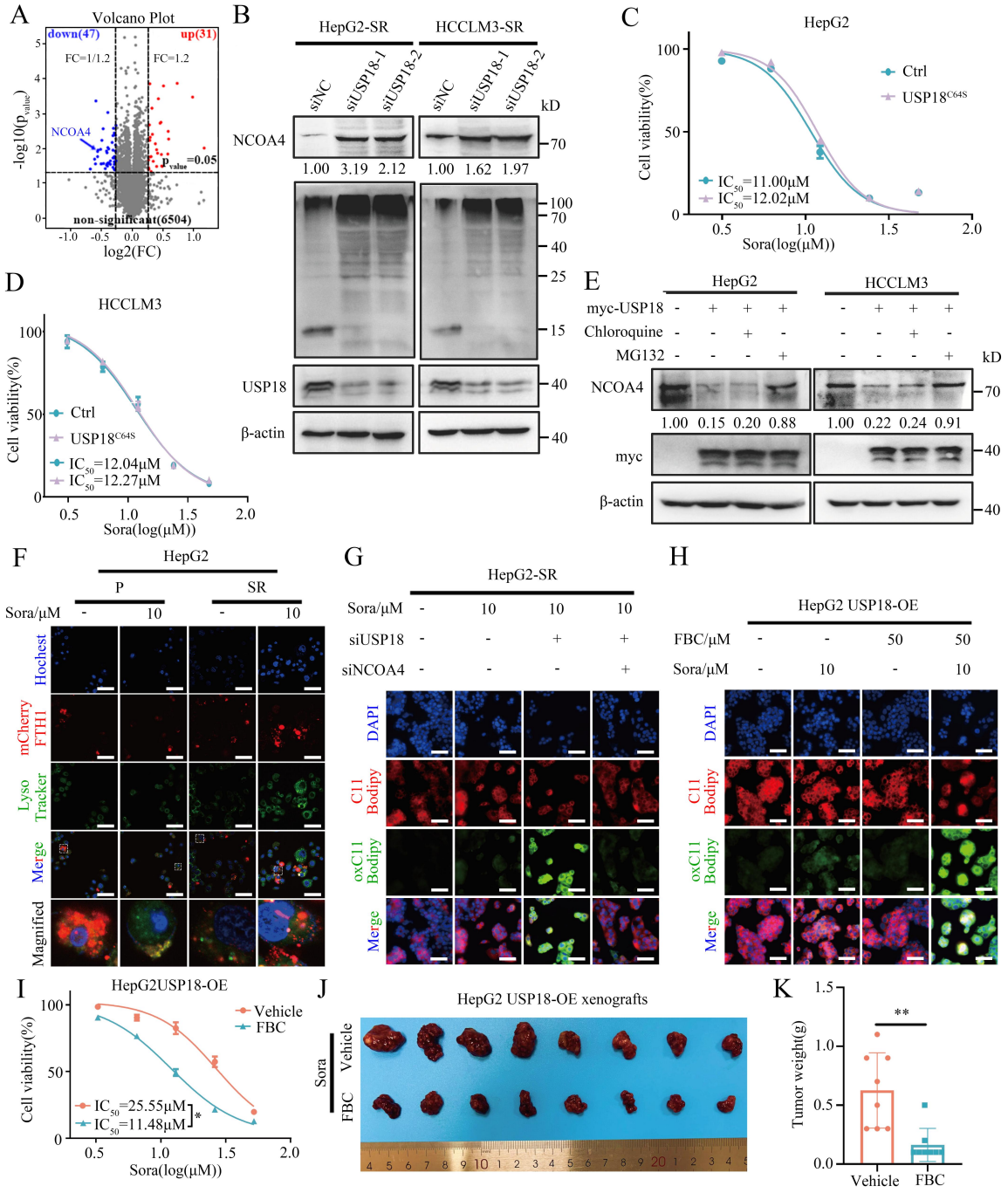

Figure S4. USP18 inhibits the sorafenib-induced ferritinophagy by decreasing NCOA4. (A) Volcano plot showing dysregulated proteins (red, up-regulated proteins; blue, down-regulated proteins) identified by proteomics

262 assays. NCOA4 was denoted by blue arrows. **(B)** Western blot analysis of
263 NCOA4 and ISG15 protein levels in HCC-SR cells transfected with or without
264 USP18 siRNAs for 48 h. The intensities of bands were analyzed by Image J and
265 normalized to the group transfected with siNC. **(C, D)** CCK-8 assay. The impact
266 of $USP18^{C64S}$ overexpression on the susceptibility of HCC cells toward sorafenib
267 treatment. **(E)** HepG2 and HCCLM3 cells were transfected with myc-USP18
268 plasmid or control plasmid and were cultured for 48 h before being further
269 incubated with MG132 (10 μM) for 4 h or chloroquine (25 μM) for 6 h. The
270 NCOA4 protein levels of the transfected cells were detected by western blot. **(F)**
271 NCOA4-mediated ferritinophagy in HepG2-P and HepG2-SR cells was assessed
272 by examining the co-localization of transferrin FTH1 with lysosomes. Scale bars,
273 5 μm. **(G)** BODIPY 581/591 C11 staining. The impact of USP18 knockdown on
274 the sorafenib-induced elevation of lipid peroxidation in HepG2-SR cells, with or
275 without NCOA4 siRNA transfection. **(H)** BODIPY 581/591 C11 staining. The
276 combined treatment of FBC and sorafenib on the sorafenib-induced elevation of
277 lipid peroxidation in HepG2 USP18-OE cells. Scale bars, 5 μm. **(I)** CCK-8 assay.
278 The influence of FBC on the susceptibility of HepG2 USP18-OE cells towards
279 sorafenib treatment (means ± SEM, *$p < 0.05$, paired student's t-test). **(J)**
280 Representative pictures of subcutaneous HepG2-USP18-OE xenografts from the
281 indicated groups (n = 8 mice per group). **(K)** The tumor weights from the
282 indicated groups (means ± SEM, **$p < 0.01$, unpaired student's t-test). n = 8 mice
283 per group.

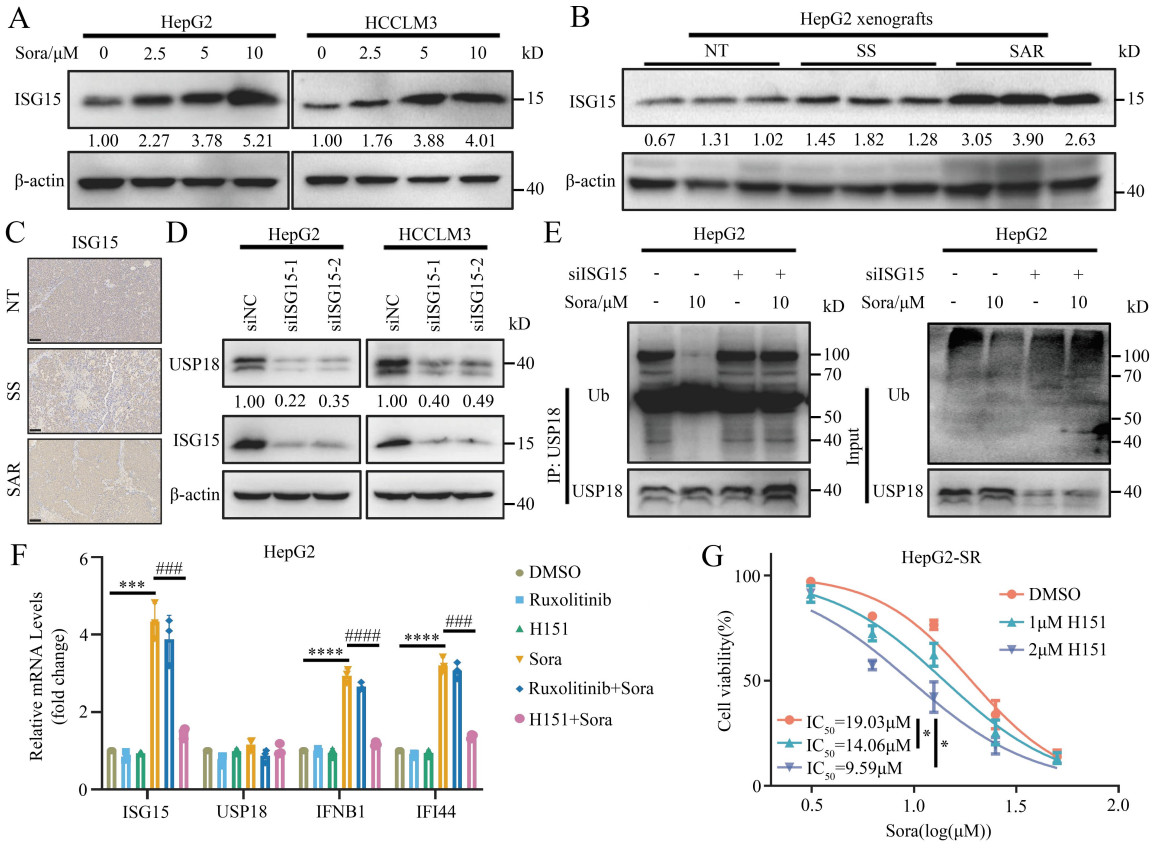

Figure S5. Sorafenib promotes USP18 accumulation via STING/IRF3/ISG15 axis in HCC cells. (A) Protein expression of ISG15 in HCC cells treated with indicated concentrations of sorafenib for 24 h. The band intensities were quantified using Image J and normalized to the control cells treated with DMSO. **(B)** Protein expression of ISG15 in the HepG2 xenografts from the indicated groups. The intensities of bands were analyzed by Image J and normalized to the mean of the corresponding NT group. **(C)** Representative IHC images of ISG15 in excised xenografts from the indicated groups. Scale bars, 50 μm. **(D)** Protein expression of USP18 in HCC-SR cells after transfection with or without ISG15 siRNA for 48 h. The intensities of bands were analyzed by Image J and

295 normalized to the group transfected with siNC. **(E)** Expression of USP18
296 ubiquitination in anti-USP18 immunoprecipitation and whole-cell lysates (input)
297 derived from HepG2 cells transfected without or with ISG15 siRNA for 48 h and
298 treated with sorafenib for 24 h. All protein samples were pretreated with 10 μM
299 MG132 for 4 hours prior to collection. *, heavy chain. **(F)** The mRNA expression
300 of downstream target genes regulated by IRF3 in HepG2 cells treated with
301 specified concentrations of Sorafenib, JAK inhibitor (Ruxolitinib), and/or STING
302 inhibitor (H151) for 24 hours was investigated. (***$p < 0.001$ and ****$p < 0.0001$
303 versus DMSO group, ###$p < 0.001$ and ####$p < 0.0001$ versus sorafenib (Sora)
304 group, one-way ANOVA test). **(G)** CCK-8 assay. The impact of STING inhibitor
305 (H151) on the susceptibility of HepG2-SR cells to sorafenib (means ± SEM, *$p <$
306 0.05, one-way ANOVA test).

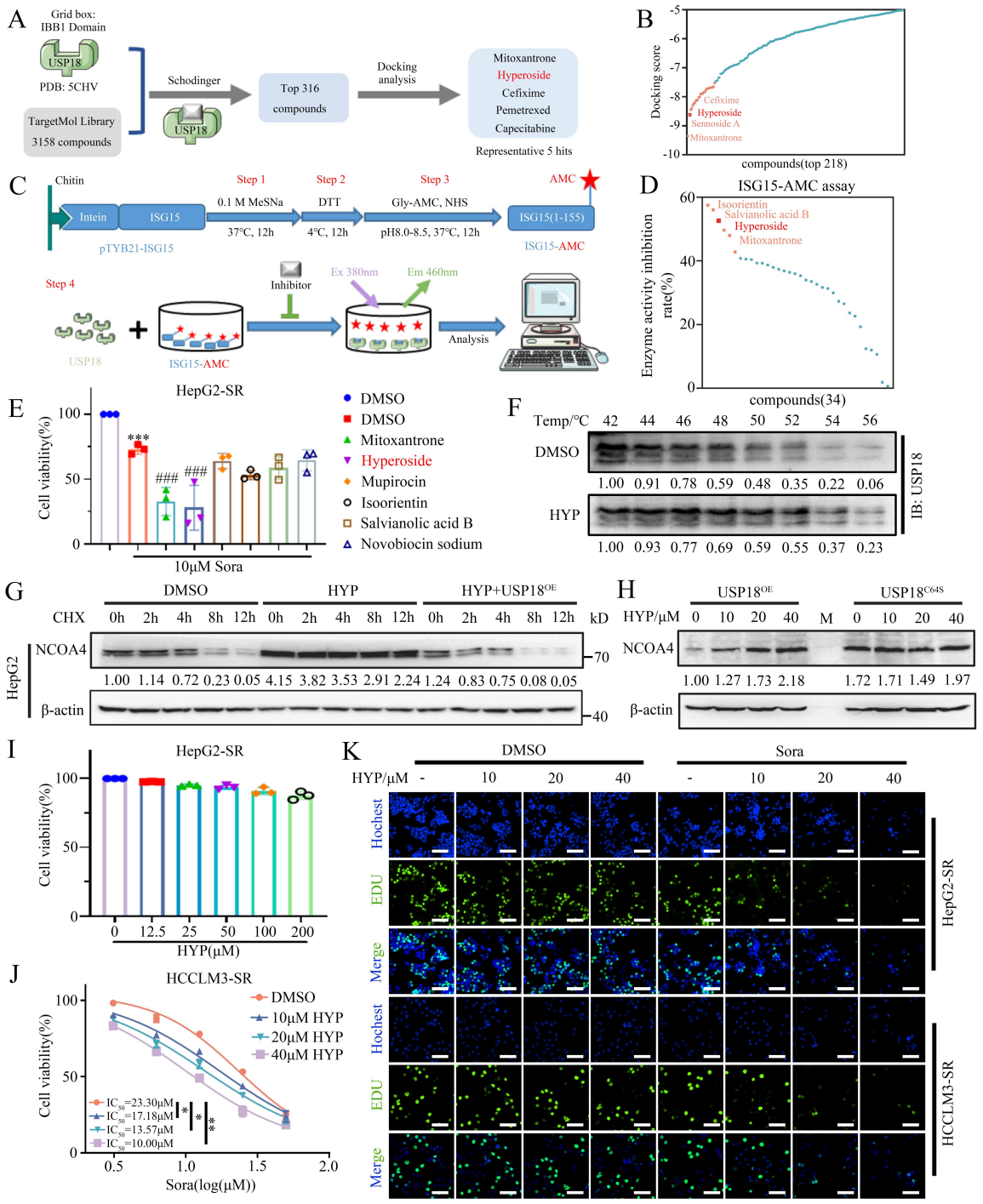

Figure S6. Identification and characterization of HYP as a USP18 inhibitor that directly targets the USP18 IBB1 domain. (A) Schematic overview of the high throughput virtual screening approach used for USP18 inhibitor identification.

311 **(B)** The depictions of molecular docking outcomes are illustrated, where
312 compounds demonstrating docking scores below 7.5 are indicated by the rose
313 red squares. **(C)** Schematic diagram of the synthesis and hydrolysis experiments
314 of ISG15-AMC. **(D)** The outcomes of the ISG15-AMC hydrolysis assay.
315 Compounds exhibiting a USP18 enzyme activity inhibition rate exceeding 40%
316 are denoted by rose red dots. **(E)** HepG2-SR cells were treated with 10 μM
317 sorafenib and 20 μM the indicated compounds for 24 h, the cell viability was then
318 measured by CCK-8 assay (means ± SEM, ***$p < 0.001$ versus DMSO group,
319 ###$p < 0.001$ versus sorafenib (Sora) group, one-way ANOVA test). **(F)** Cellular
320 thermal shift assay (CETSA) was used to evaluate the binding between HYP and
321 USP18 in thermodynamic levels. The expression of USP18 was detected by
322 western blot. **(G)** HepG2 cells were transfected with either myc-USP18 plasmid
323 or control plasmid for 48 hours, and then cultured with DMSO or 40 μM HYP for
324 24 hours before further incubation with CHX for 0, 2, 4, 8, and 12 hours. The
325 NCOA4 protein levels in each group of cells were detected by Western blotting.
326 **(H)** The impact of HYP on the expression level of NCOA4 protein in $USP18^{OE}$ or
327 $USP18^{C64S}$ stable cell lines was investigated using WB analysis. **(I)** CCK-8 assay.
328 The impact of HYP on the cell viability of HepG2-SR cells. **(J)** CCK-8 assay. The
329 impact of HYP on the susceptibility of HCCLM3-SR cells to sorafenib (means ±
330 SEM, *$p < 0.05$, **$p < 0.01$, one-way ANOVA test). **(K)** EDU assay. The impact of
331 HYP on the proliferation of HCC-SR cells toward sorafenib treatment. Scale bars,
332 5 μm.

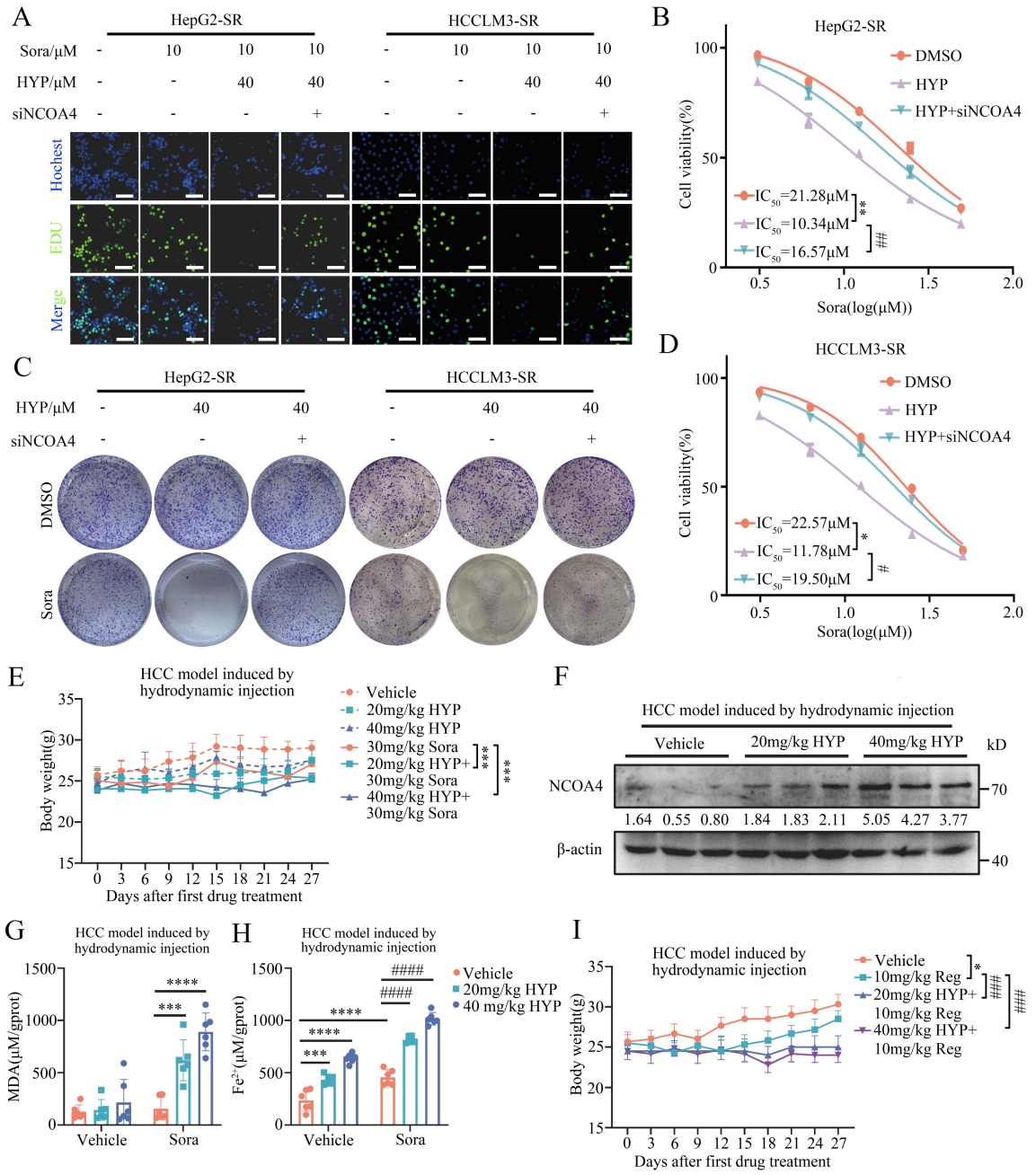

Figure S7. HYP enhances the sensitivity of HCC-SR cells to sorafenib by upregulating NCOA4. (A, B and D) HCC-SR cells were transfected with siNC or siNCOA4 for 48 h and treated with 10 μM sorafenib and/or 40 μM HYP for 24 h. The proliferation cells were analyzed by EDU assay (A). Scale bars, 5 μm. The

338 cell viability was measured by CCK-8 assay (B and D) (means ± SEM, *p < 0.05,
339 **p < 0.01 versus DMSO, #p < 0.05, ##p < 0.01 versus HYP, paired student's t-
340 test). **(C)** Colony formation assay. HCC-SR cells were transfected with or without
341 NCOA4 siRNA for 48 h and treated with 10 μM sorafenib and/or 40 μM HYP for
342 24 h in complete media, washed with PBS, and cultured in complete media for
343 another 14 days. **(E)** The body weights of the indicated groups (means ± SEM,
344 ***p < 0.001 versus 30mg/kg Sora group, one-way ANOVA test). **(F)** Protein
345 expression of NCOA4 in HCC model induced by hydrodynamic injection from the
346 indicated groups. **(G, H)** Detection of MDA content and Fe^{2+} level in the indicated
347 groups of hepatocellular carcinoma model induced by hydrodynamic injection
348 (means ± SEM, ***p < 0.001, ****p < 0.0001 versus Vehicle group, ###p < 0.001,
349 ####p < 0.0001 versus 30mg/kg Sora group, one-way ANOVA test). **(I)** The body
350 weights of the indicated groups (means ± SEM, *p < 0.05 versus Vehicle group,
351 ###p < 0.001 versus 30mg/kg Sora group, one-way ANOVA test).